

Gas-phase synthesis of SWNT by an atmospheric pressure plasma jet

O. Smiljanic^{a,*}, B.L. Stansfield^a, J.-P. Dodelet^a, A. Serventi^a, S. Désilets^b

^a *Institut National de la Recherche Scientifique (INRS), Energie et Matériaux, 1650, boulevard Lionel Boulet, Varennes, Que., Canada J3X 1S2*

^b *CRDV, 2459 boul Pie-XI Nord, Val-Bélair, Que., Canada G3J 1X5*

Received 28 September 2001; in final form 22 January 2002

Abstract

We present here a new method for producing single wall carbon nanotubes (SWNT) based on the atomization of a gaseous mixture (composed of argon, ferrocene and ethylene) in an atmospheric plasma jet. Scanning electron microscopy (SEM), high-resolution transmission electron microscopy (HR-TEM) and Raman spectroscopy were performed to study the samples obtained. They contain SWNT with diameters and structure comparable to those produced by laser ablation and arc discharge techniques. Since this method is continuous and easily scalable, we feel it has potential for large-scale commercial production of SWNT. © 2002 Elsevier Science B.V. All rights reserved.

1. Introduction

Because of their exceptional properties [1], single wall carbon nanotubes (SWNT) are predicted to have important applications in many fields, such as hydrogen storage [2,3], material reinforcement [4], and nanotechnology [5]. However, the problems of cost and availability of sufficiently large quantities of SWNT limit the level of research and particularly the development of any industrial application. To date, laser ablation, arc discharge and CVD are the most popular methods used for the synthesis of SWNT [1]. Laser ablation

and arc discharge techniques are based on the same basic principle: the plasma produced by the local evaporation of a metal-enriched graphite rod condenses in the form of SWNT, metal nanoparticles and amorphous carbon. The growth mechanism is not completely understood, but it can be considered to follow these steps [6]. Although the conversion of graphite to SWNT is very efficient with these techniques, they fail to provide SWNT at low cost, because the vaporization of graphite is energy-consuming and these methods are not continuous. Finally, in the CVD technique, a gas is passed over metal nanoparticles (typically iron, cobalt, nickel or their mixtures) from which the tubes grow. Unfortunately, this approach is limited by the encapsulation of the catalyst and the diffusion of carbon through the metal particle [7], which stops the growth process and prevents high

* Corresponding author. Fax: 450-929-8102.

E-mail address: smiljani@inrs-ener.quebec.ca (O. Smiljanic).

yields. The catalyst is seen to play a key role in all SWNT production methods.

In our method, we try to reproduce the conditions prevailing in the arc discharge and laser ablation approaches, but a carbon-containing gas is used instead of graphite vapors to supply the carbon necessary for the production of SWNT. Doing so, the growth of SWNT is more efficient. It is also continuous and occurs at low cost. To produce a continuous process, a gas mixture composed of argon, ethylene and ferrocene is introduced into a microwave plasma torch, where it is atomized by the atmospheric pressure plasma, which has the form of an intense ‘flame’. The fumes created by the flame are found to contain SWNT, metallic and carbon nanoparticles and amorphous carbon.

2. Experimental

Our method is based on the atomization of a gaseous mixture by an atmospheric-pressure microwave plasma torch. A schematic overview of the system is presented in Fig. 1. Microwaves are generated by a magnetron from a domestic microwave oven (1300 W) supplied by a DC current. The microwave radiation travels inside a copper waveguide, which is short-circuited at one end by a metallic plate. A boron nitride or quartz tube with a 13 mm inner diameter serves as the ‘plasma tube’ and traverses the waveguide at a position a quarter wavelength upstream from the short-circuit. The plasma flame is sustained by the microwave radi-

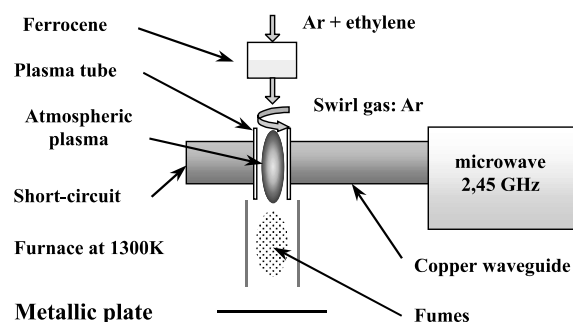


Fig. 1. Schematic drawing of the system. The samples are collected on the metallic plate and in the plasma tube.

ation and confined inside the plasma tube. It is kept from attaching to the walls by a swirl jet of argon. The carbon-containing gas (ethylene) and the catalyst in the form of ferrocene are introduced by an axial flow. Ferrocene vapor obtained by a temperature-controlled sublimation is entrained by an inert gas (argon). The maximum introduction rate of ferrocene is 50 mg/min and the ethylene throughput ranges between 0 and 200 sccm. Ferrocene has already been used by some authors as metal precursor for the production of carbon nanotubes [8–10]. A temperature measurement of the plasma with this gas mixture was not performed, but results reported by Woskov et al. [11] give a good indication. In their experiments, a nitrogen plasma operated under similar conditions had a temperature of 5500 ± 500 K. The exhaust from the plasma tube is fed into a larger diameter (34 mm) quartz tube, placed inside a tubular furnace whose temperature is maintained at 1300 K in order to prevent an excessively large temperature gradient at the outlet of the torch, which could lead to the formation of amorphous carbon. The temperature of the furnace was measured with a pyrometer. Deposits are formed in the plasma tube, and on the horizontal cold metallic plate at the exit of the furnace, from which it could be peeled off. The quartz tube inside the furnace is free of any deposit. The samples were studied by scanning and high-resolution transmission electron microscopies (SEM and HR-TEM) and Raman spectroscopy. The SEM is a JEOL JSM-6300F, and the TEM is a Hitachi H-9000 NAR high-resolution microscope operated at 300 kV. The Raman spectra were taken with a Renishaw 3000 using 514.5 nm Ar^+ laser radiation in the backscattering geometry.

3. Results and discussion

The results presented here and the discussion are based on ‘as produced’ (unpurified) samples. In Figs. 2a and b, we show scanning electron micrographs of the samples found on the metallic plate at the exit of the furnace. Indeed, the raw sample is essentially composed of bundles of SWNT, mixed with amorphous carbon particles.

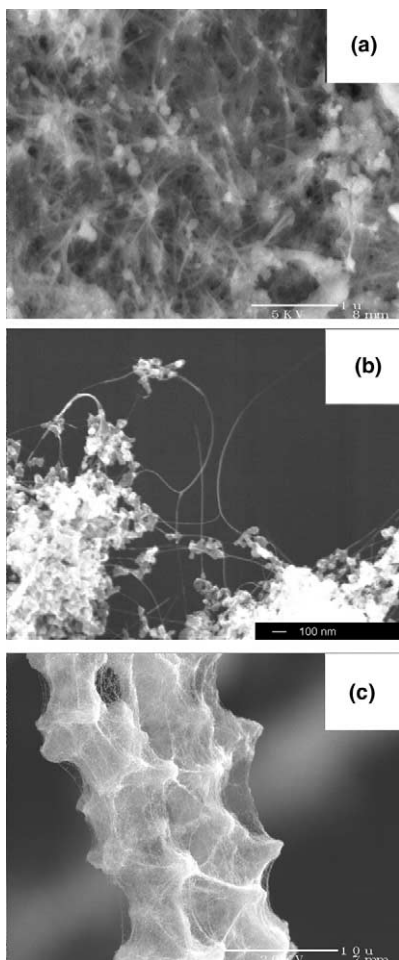


Fig. 2. Scanning electron micrographs of the samples taken from three different places: two different regions on the metallic plate ((a) and (b)), and in the plasma tube (c).

SWNT bundles with diameters of approximately 20 nm and more than 3 μm long are illustrated in Fig. 2b. The clusters of amorphous carbon particles are more evident in this image, which suggests that the conditions for the formation of SWNT may vary within the torch or at its immediate exit. It is known, for example, that the diameter of the nanotubes is a function of the temperature [12]. In our case, it is inevitable that the quality of the product will depend strongly on the ability of the plasma to dissociate the carbon-containing gas. Indeed, a carbon deposit forms on the inner walls of the plasma tube during the experiment. Fig. 2c

shows an overview of this structure; this black deposit is essentially composed of web-like ‘stalactites’ rooted on the surface of the tube, extending into the plasma flame. TEM measurements show that the web is composed of SWNT intermingled with aggregates of metallic nanoparticles (10–100 nm) coated with carbon. These stalactites have good mechanical strength, as they can be picked up from the plasma tube with a pair of tweezers without breaking. On the other hand, this deposit prevents a good coupling between the microwaves and the plasma, resulting in a degradation of the plasma with time (the flame extinguishes after 15–20 min). Results indicate, however, that an optimization of the process could lead to relatively clean SWNT deposits.

A TEM image displayed in Fig. 3 shows clearly that the nanotubes produced are SWNT with diameters of approximately 1.5 nm. As in Figs. 2a and b, the tubes are surrounded by a matrix composed of amorphous carbon and metallic nanoparticles having diameters between 1 and 3 nm as shown on the left of the TEM micrograph. Thus, the catalyst nanoparticles needed for the

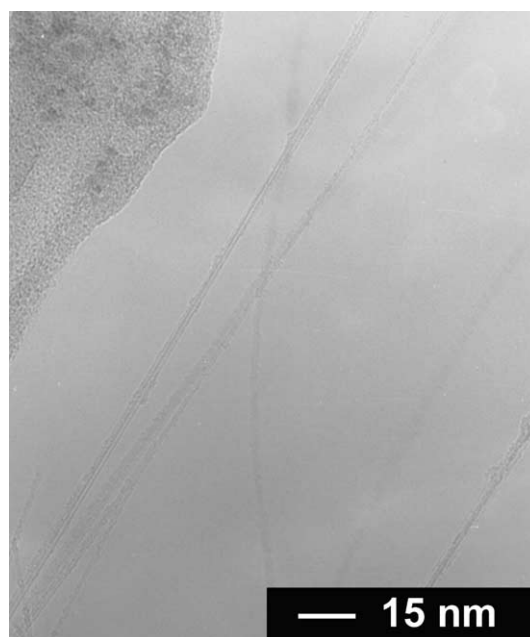


Fig. 3. High-resolution transmission electron micrograph of pristine SWNT deposited on the metallic plate.

formation of the tubes are seen to be spontaneously created by the process. In order to determine more precisely the spread in tube diameters obtained with this method, Raman spectroscopy was performed in different regions of the sample. The spectra show good agreement with previous observations made on SWNT [13]. The peaks around 1585 cm^{-1} are associated with the graphitic nature of the tubes, and the broad peak around 1350 cm^{-1} indicates the disorder in the sample due to carbon nanoparticles and the random orientation of the tubes [1]. In order to determine the average diameter of the tubes, we focus on the low frequency region (between 100 and 300 cm^{-1}), where the tube diameter can be related to the frequency shift by the following relation [12]:

$$\nu\text{ (cm}^{-1}\text{)} = \frac{223.75\text{ (nm cm}^{-1}\text{)}}{d\text{ (nm)}},$$

where ν is the frequency of the A_{1g} radial breathing mode (RBM) of the tube and d is the diameter of the tube. The RBM is strongest in the low frequency region, which makes it possible to make a direct correspondence between the frequency shift of the peak and the diameter of the tubes [12,14]. There is a shift between the peaks obtained from pristine SWNT and those from bundles [14]; in the latter case 15 cm^{-1} has to be added to the preceding relation to fit the data obtained with bundles. Since we observed a majority of isolated SWNT by HR-TEM, we decided to use the relation without the correction. From the Raman spectrum of the sample taken on the plate, represented in Fig. 4a, we can identify six peaks, at 147 , 165 , 181 , 203 , 243 , and 261 cm^{-1} , corresponding to tubes with diameters of 1.52 , 1.36 , 1.24 , 1.10 , 0.92 , and 0.86 nm , respectively. This spread in diameters contrasts with the Raman spectrum of the web-like deposit in the plasma tube, presented in Fig. 4b, where only tubes with diameters greater than 1.22 nm are present ($\nu \leq 183\text{ cm}^{-1}$). The peak at 183 cm^{-1} is strong enough in this case to make the E_{1g} translational mode (observed at 133 cm^{-1}) visible. The other peaks at 163 and 145 cm^{-1} correspond to tubes with diameters of 1.37 and 1.54 nm , respectively. Since larger tubes have been found to be formed at higher temperatures [12], we

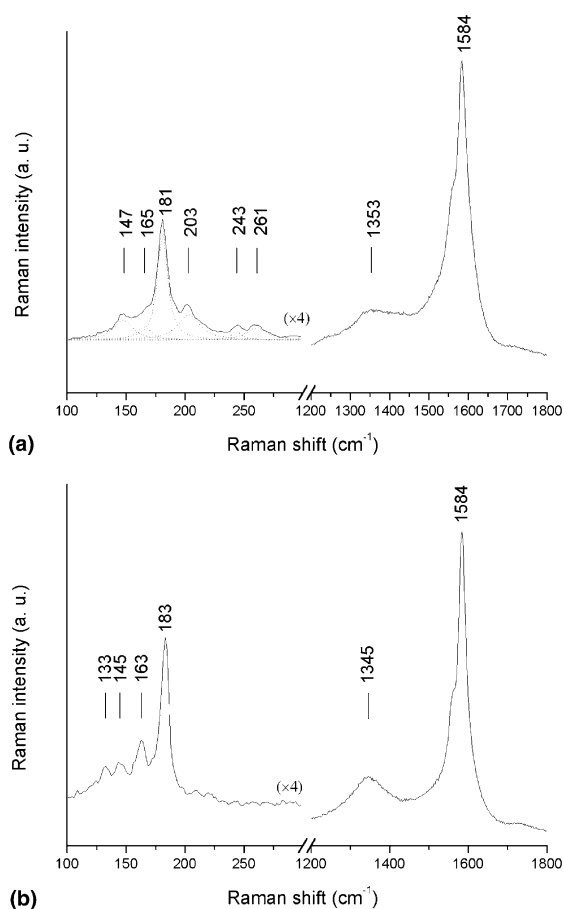


Fig. 4. Typical breathing mode and tangential mode Raman spectra of the samples taken from the metallic plate (a) and from the plasma tube (b), using 514.5 nm laser radiation.

can conclude that in the vicinity of the plasma flame, the temperature is higher than in the furnace (1300 K), enabling the formation of tubes with larger diameters. The peak around 1350 cm^{-1} is also sharper in Fig. 4b than in Fig. 4a, indicating that the higher temperature in the plasma tube may be responsible for the formation of less disordered carbon than in the sample found on the plate.

These results show that our gas-phase method can produce SWNT comparable in quality, purity and aspect ratio to those produced by the laser ablation and arc discharge techniques. Although Ando et al. [15] proposed an approach based on an

arc plasma jet supplied with metal-enriched graphite, feeding the reaction with a carbon-containing gas rather than vaporizing graphite is advantageous in many ways. On one hand, the process can be continuous and is, in principle, easily scalable to produce large quantities of SWNT. On the other hand, the energy cost is lowered: 716.7 kJ are needed to atomize a mole of graphite, compared to 52.3 kJ/mol liberated by ethylene. It is important to stress that in our experiment the catalyst is iron, which is supposed to be a relatively poor catalyst for the growth of SWNT [16]. On the other hand, the advantages of using ferrocene as iron precursor are its innocuity and low cost. One of the clues to explaining these good results with iron is the presence of hydrogen, which is known to be a growth promoter for nanotubes produced via CVD [4]. As a matter of fact, acetylene and methane were also tested in the process. In the first case, only traces of SWNT were present, whereas methane gave quantities of SWNT comparable to those produced using ethylene. The fact that in acetylene, the hydrogen-to-carbon atomic ratio is equal to 1 while for ethylene and methane it is equal to 2 and 4, respectively, suggests that the presence of hydrogen is important for the formation of SWNT by this technique. Because of the cost and/or toxicity of cobaltocene and nickelocene, these metal precursors were not tested as catalysts, and, in fact, it is difficult to imagine a large-scale production of SWNT based on a catalyst made from a suspected cancerous agent precursor-like nickelocene.

4. Conclusion

We report here the production of SWNT by a gas-phase method using iron as the catalyst, which provides results comparable to laser ablation and arc discharge techniques. The study of the sample by electron microscopy and Raman spectroscopy confirmed the presence of SWNT both in bundles and isolated with diameters ranging from approximately 0.9 to 1.5 nm. The process is not yet optimized, but once the problem of carbon depo-

sition in the plasma tube has been solved, quantitative analyses will be made. This method is promising in its simplicity and the possibility of achieving continuous production of SWNT.

Acknowledgements

The authors would like to thank C. Côté, F. Larouche, G. Lebrun and P. Noël for helpful discussions and invaluable help with the experiments.

References

- [1] R. Saito, G. Dresselhaus, M.S. Dresselhaus, *Physical Properties of Carbon Nanotubes*, Imperial College Press, London, 1998.
- [2] C. Liu, Y.Y. Fan, M. Liu, H.T. Cong, H.M. Cheng, M.S. Dresselhaus, *Science* 286 (1999) 1127.
- [3] M.S. Dresselhaus, K.A. Williams, P.C. Eklund, *MRS Bull.* (1999) 45.
- [4] P.J.F. Harris, *Carbon Nanotubes and Related Structures*, Cambridge University Press, Cambridge, 1999.
- [5] M. Menon, D. Srivastava, *Phys. Rev. Lett.* 79 (1997) 4453.
- [6] A.A. Puzos, D.B. Geohegan, S.J. Pennycook, *Appl. Phys. A* 70 (2000) 153.
- [7] J.H. Hafner, M.J. Bronikowski, B.R. Azamian, P. Nikolaev, A.G. Rinzler, D.T. Colbert, K.A. Smith, R.E. Smalley, *Chem. Phys. Lett.* 296 (1998) 195.
- [8] R.L. Vander Wal, T.M. Tichich, V.E. Curtis, *Chem. Phys. Lett.* 323 (2000) 217.
- [9] B.C. Satishkumar, A. Govindaraj, R. Sen, C.N.R. Rao, *Chem. Phys. Lett.* 293 (1998) 47.
- [10] H.M. Cheng, F. Li, G. Su, H.Y. Pan, L.L. He, X. Sun, M.S. Dresselhaus, *Appl. Phys. Lett.* 72 (1998) 3282.
- [11] P.P. Woskov, K. Hadidi, M.C. Borrás, P. Thomas, K. Green, G.J. Flores, *Rev. Sci. Instrum.* 70 (1999) 489.
- [12] A.M. Rao, S. Bandow, E. Richter, P.C. Eklund, *Thin Solid Films* 331 (1998) 141.
- [13] A.M. Rao, E. Richter, S. Bandow, B. Chase, P.C. Eklund, K.A. Williams, S. Fang, K.R. Subbaswamy, M. Menon, A. Thess, R.E. Smalley, G. Dresselhaus, M.S. Dresselhaus, *Science* 275 (1997) 187.
- [14] Z. Yu, L. Brus, *J. Phys. Chem. B* 105 (2001) 1123.
- [15] Y. Ando, X. Zhao, K. Hirahara, K. Suenaga, S. Bandow, S. Iijima, *Chem. Phys. Lett.* 323 (2000) 580.
- [16] M. Yudasaka, R. Yamada, N. Sensui, T. Wilkins, T. Ichihashi, S. Iijima, *J. Phys. Chem. B* 103 (1999) 6224.